Simulating Spin-Echo MRI Signal Contrast Response to T_R–T_E Variations in Tissues with Spatially Varying T_1–T_2 Maps

Renato III F. Bolo,[a,*] Aldrin James R. Garcia,[a] Mariane R. Madlangsakay,[a] Crisleo John II E. Martinito,[a] Katlyn Faye B. Nacague,[a] and Herbert B. Domingo[a]

[a]*Department of Physical Sciences and Mathematics, University of the Philippines Manila*
[*]Corresponding author: rfbolo@up.edu.ph

Abstract

Perspiciatis unde omnis iste natus error sit voluptatem accusantium doloremque laudantium, totam rem aperiam, eaque ipsa quae ab illo inventore veritatis et quasi architecto beatae vitae dicta sunt explicabo. Nemo enim ipsam voluptatem quia voluptas sit aspernatur aut odit aut fugit, sed quia consequuntur magni dolores eos qui ratione voluptatem sequi nesciunt. Neque porro quisquam est, qui dolorem ipsum quia dolor sit amet, consectetur, adipisci velit, sed quia non numquam eius modi tempora incidunt ut labore et dolore magnam aliquam quaerat voluptatem. Ut enim ad minima veniam, quis nostrum exercitationem ullam corporis suscipit laboriosam, nisi ut aliquid ex ea commodi consequatur? Quis autem vel eum iure reprehenderit qui in ea voluptate velit esse quam nihil molestiae consequatur, vel illum qui dolorem eum fugiat quo voluptas nulla pariatur?

Keywords: keyword 1, keyword 2

1 Statement of the Problem

Magnetic Resonance Imaging (MRI) is a non-invasive diagnostic technique widely used in clinical and research settings for its ability to produce detailed anatomical and functional images without ionizing radiation. The contrast in MRI images is fundamentally governed by intrinsic tissue parameters, primarily the longitudinal relaxation time (T_1) and the transverse relaxation time (T_2) [1]. These parameters reflect how different tissues return to equilibrium after perturbation by radiofrequency (RF) pulses and are critical to understanding signal formation. The time evolution of the net magnetization vector in response to RF excitation and relaxation processes is described by the Bloch equations [2].

In particular, spin-echo sequences—common in both clinical and research MRI—yield a steady-state solution to the Bloch equations that relates signal intensity to T_1, T_2, repetition time (T_R), and echo time (T_E) [3]. This steady-state solution forms the basis for simulating and interpreting MRI contrast. Most introductory and educational simulations rely on simplifying assumptions, including the notion that tissue compartments are homogeneous in their relaxation properties. However, this abstraction oversimplifies the complexity of biological tissues, especially under pathological conditions.

Although T_1 and T_2 describe intrinsic tissue characteristics, the imaging parameters T_R and T_E play an equally crucial role in shaping the observed signal contrast. The choice of T_R governs the extent of longitudinal recovery between excitations, while T_E determines how much transverse signal decay is captured at readout. Together, these timing parameters modulate sensitivity to different tissue types and heterogeneities. As such, understanding the interaction between T_1, T_2, T_R, and T_E is essential not only for optimizing contrast but also for interpreting variations in signal intensity in regions where relaxation times vary spatially [3].

In reality, tissues often exhibit intra-regional heterogeneity in relaxation parameters due to variations in cellularity, water content, perfusion, necrosis, or other microstructural and physiological processes [4]. For instance, tumors may contain a mixture of viable cells, necrotic cores, and edematous regions, each with subtly different T_1 and T_2 values. While these variations may not produce overt visual differences in standard MR images, they influence the local signal response and can affect both qualitative and quantitative interpretations of the image.

This project focuses on understanding how spatial variations in T_1 and T_2 values within a single tissue region impact the resulting MRI signal, using numerical simulations grounded in the steady-state Bloch model. By going beyond homogeneous-tissue models, the study seeks to explore the degree to which intra-regional relaxation heterogeneity affects signal intensity and image contrast. Such insights are relevant for both medical imaging applications, where accurate tissue characterization is essential, and fundamental physics, where a detailed understanding of signal formation informs the design and interpretation of MR experiments.

2 General Purpose of the Study

The purpose of this study is to simulate and analyze how spatial heterogeneity in T_1 and T_2 relaxation times within a tissue region influences MRI signal contrast, using the steady-state solution to the Bloch equations under spin-echo imaging conditions.

3 Specific Objectives

To accomplish this, the study specifically aims to:

1. Derive and implement the steady-state signal expression for a spin-echo MRI sequence based on the Bloch equations;

2. Encode spatial variation in T_1 and T_2 relaxation parameters across a 2D tissue model with a lesion region; and

3. Generate and analyze synthetic contrast maps to assess the effect of intra-lesion relaxation gradients on MRI signal intensity.

4 Review of Related Literature

Magnetic Resonance Imaging (MRI) leverages the relaxation properties of nuclear spins—longitudinal (T_1) and transverse (T_2)—to generate high-contrast images of soft tissues without ionizing radiation. The time evolution of magnetization under these relaxation processes is governed by the Bloch equations [2], forming the theoretical foundation of MRI. In the context of spin-echo sequences, the steady-state signal intensity can be described as

$$S(x,y) = \rho \left[1 - e^{-TR/T_1(x,y)} \right] e^{-TE/T_2(x,y)}, \tag{1}$$

where ρ is the proton density, and TR and TE are the repetition and echo times, respectively [3]. This formulation provides a direct quantitative relationship between tissue-specific relaxation parameters and image contrast [1].

Relaxation times vary significantly between tissue types and are influenced by imaging parameters and magnetic field strength. For example, Stanisz et al. [5] measured T_1 values in gray matter at 1.5 T, which is a widely used field strength for modern MRI machines [1], to be within the range 1124 ± 50 ms, and T_2 values between 95 ± 8 ms. Bojorquez et al. [6] further demonstrated that acquisition protocols and scanner-specific settings introduce substantial variability, highlighting the importance of reproducibility in clinical interpretation. Moreover, pathologies such as tumors often exhibit altered relaxation profiles due to changes in water content, cellular architecture, or necrosis, as noted in Tofts' review of quantitative MRI in disease states [4].

Emerging work has shown that spatial heterogeneity in relaxation parameters can meaningfully affect image contrast. Does et al. [7] observed multicomponent T_1 relaxation in rat brain tissue, attributing the behavior to underlying microstructural variations. Xu et al. [8] similarly showed that T_2 variability affects the accuracy of diffusion-weighted imaging, emphasizing the clinical impact of intra-tissue relaxation differences. Despite this, many MRI models assume homogeneity across regions of interest, which may limit their realism in depicting diseased tissues.

Efforts to standardize quantitative MRI across platforms have underscored persistent challenges. A recent multi-center study using the NIST/ISMRM phantom reported inter-scanner variability in T_1 and T_2 under 7%, but confirmed that minor discrepancies can still affect quantitative outcomes [9]. Furthermore, myocardial studies by Wiesmüller et al. [10] revealed notable intra-segmental T_2 variation even under consistent imaging conditions, thus underscoring the importance of incorporating spatial gradients in modeling signal formation.

Computational simulations using the Bloch equations offer a tractable framework for exploring these phenomena under controlled conditions. Recent tools such as `BlochSim.jl` [11] and other open-source packages for MRI signal modeling provide accessible environments for simulating magnetization dynamics, but typically assume spatial uniformity in tissue parameters. As such, simulations incorporating spatially varying T_1 and T_2 maps remain underutilized, despite their potential to visualize how subtle tissue gradients manifest as signal heterogeneity.

While spatial heterogeneity in T_1 and T_2 presents a crucial dimension in tissue modeling, the interplay between these relaxation parameters and acquisition settings—particularly the repetition time (TR) and echo time (TE)—also fundamentally shapes signal behavior. Optimal selection of TR and TE is essential for maximizing lesion conspicuity and diagnostic performance. Hendrick et al. [12] demonstrated,

Guided Research on the Physics of MRI
Submitted in Partial Fulfillment of Requirements in APHYSICS 191
University of the Philippines Manila, Padre Faura St., Manila, August 2025

2

through Bloch-equation modeling, that CNR in spin-echo MRI is sensitive to interpulse delays, identifying parameter regimes that maximize signal discrimination between tissues.

More recently, Ragot and Chen [13] challenged the assumption that $TE = T_2$ yields maximal contrast, showing via physiological-noise modeling that shorter echo times (around 50 ms at 3T) often outperform nominal T_2-matching in terms of CNR. Furthermore, the concept of lesion-to-background contrast ratio (LBCR) has gained traction in clinical studies as a robust proxy for lesion detectability, though optimization of TR and TE specifically for LBCR in spin-echo imaging remains underexplored. These findings underscore the need to account for both spatially varying tissue properties and acquisition parameter sensitivity when modeling MRI signal formation.

In summary, while theoretical models and standardization phantoms have greatly improved our understanding of MRI contrast, there remains a gap in simulating how smooth spatial variations in relaxation parameters within lesions influence signal intensity under spin-echo conditions. This study addresses that gap by implementing voxel-wise relaxation maps within a 2D phantom, providing insight into the interplay between tissue heterogeneity and MRI signal behavior as a step toward bridging simplified simulations and the complex biological realities of clinical imaging.

5 Methodology

5.1 Overview

This project simulates the MRI signal produced by a tissue slice with spatially varying relaxation times under a spin-echo pulse sequence. A 2D matrix (phantom) will be used to represent a 25-pixel cross-sectional slice, where the background tissue is homogeneous gray matter and a circular lesion is embedded at the center. While the background will have fixed longitudinal and transverse relaxation values (T_1, T_2), the lesion region will exhibit radial gradients in both parameters, simulating intra-lesion heterogeneity.

The net magnetization vector $\mathbf{M}(t)$ evolves according to the Bloch equations:

$$\frac{d\mathbf{M}}{dt} = \gamma \mathbf{M} \times \mathbf{B} - \begin{bmatrix} M_x/T_2 \\ M_y/T_2 \\ (M_z - M_0)/T_1 \end{bmatrix} \tag{2}$$

where γ is the gyromagnetic ratio, $\mathbf{B}$ is the effective magnetic field, and M_0 is the equilibrium magnetization. For this simulation, we consider the steady-state signal under a spin-echo imaging sequence.

5.2 Signal Equation (Spin-Echo)

In a conventional spin-echo (SE) imaging sequence with repeated radiofrequency (RF) excitations, the observable signal intensity at each voxel (x, y) can be modeled. After an initial transient period, the longitudinal magnetization reaches a dynamic equilibrium. If the repetition time (TR) is sufficiently long for the transverse magnetization to decay to zero before the next RF pulse, the system is said to be in a steady-state incoherent (SSI) condition.

To simplify the derivation of the steady-state spin-echo signal, we make the following common assumptions:

1. The derivation is performed in a rotating frame of reference that precesses at the Larmor frequency, which simplifies the precession term in the Bloch equations and makes the effects of RF pulses easier to visualize.

2. RF pulses (90° and 180°) are assumed to be instantaneous, meaning they rotate the magnetization without any relaxation occurring during the pulse itself.

3. The 90° pulse perfectly rotates M_z to M_{xy}, and the 180° pulse perfectly flips M_{xy} and M_z.

4. The steady-state incoherent (SSI) condition is considered, where any residual transverse magnetization from the previous repetition is assumed to have fully decayed before the next excitation pulse. This is generally valid for long TR values.

5. The effects of macroscopic motion (flow) and microscopic random motion (diffusion) on the signal are ignored.

6. A uniform proton density (ρ) is assumed throughout the tissue, which is multiplied at the end to represent the available magnetization.

Guided Research on the Physics of MRI
Submitted in Partial Fulfillment of Requirements in APHYSICS 191
University of the Philippines Manila, Padre Faura St., Manila, August 2025
3

Let the longitudinal magnetization just before the 90° excitation pulse be $M_{z,TR}^{-}$. The transverse magnetization is assumed to be zero in the steady-state incoherent case.

The 90° pulse rotates $M_{z,TR}^{-}$ into the transverse plane. So, immediately after the pulse:

$$M_{xy}(0) = M_{z,TR}^{-}$$
$$M_z(0) = 0$$

During this period, the transverse magnetization decays due to T_2 relaxation, and the longitudinal magnetization recovers due to T_1 relaxation.

$$M_{xy}(t) = M_{xy}(0) \cdot e^{-t/T_2}$$
$$= M_{z,TR}^{-} \cdot e^{-t/T_2}$$
$$M_z(t) = M_0(1 - e^{-t/T_1}) \quad \text{(since } M_z(0) = 0 \text{ and it recovers towards } M_0\text{)}.$$

At $t = TE/2$:

$$M_{xy}(TE/2) = M_{z,TR}^{-} \cdot e^{-(TE/2)/T_2}$$
$$M_z(TE/2) = M_0(1 - e^{-(TE/2)/T_1})$$

The 180° pulse rephases the transverse magnetization and inverts the longitudinal magnetization. The phase of M_{xy} is effectively flipped, but its magnitude remains unchanged by the ideal 180° pulse for the purpose of the echo formation. The dephasing that occurred is reversed.

$$M_z(TE/2)^{+} = -M_z(TE/2)^{-} = -M_0(1 - e^{-(TE/2)/T_1})$$

The transverse magnetization now rephases and continues to decay due to T_2 relaxation. The longitudinal magnetization continues to recover towards M_0. At the echo time ($t = TE$), the signal is maximum due to rephasing. The transverse magnetization at the echo (S_{echo}) is the remaining magnitude of the transverse magnetization from before the 180° pulse, now further decayed for another $TE/2$ duration.

$$S_{echo} = M_{xy}(TE/2) \cdot e^{-(TE/2)/T_2}$$
$$= (M_{z,TR}^{-} \cdot e^{-(TE/2)/T_2}) \cdot e^{-(TE/2)/T_2}$$
$$S_{echo} = M_{z,TR}^{-} \cdot e^{-TE/T_2}$$

The longitudinal magnetization M_z at $t = TE$ will recover from its inverted state:

$$M_z(TE) = M_0 + (M_z(TE/2)^{+} - M_0)e^{-(TE/2)/T_1}$$
$$M_z(TE) = M_0 + (-M_0(1 - e^{-(TE/2)/T_1}) - M_0)e^{-(TE/2)/T_1}$$
$$M_z(TE) = M_0 + (-M_0 + M_0 e^{-(TE/2)/T_1} - M_0)e^{-(TE/2)/T_1}$$
$$M_z(TE) = M_0 + (-2M_0 + M_0 e^{-(TE/2)/T_1})e^{-(TE/2)/T_1}$$
$$M_z(TE) = M_0 - 2M_0 e^{-(TE/2)/T_1} + M_0 e^{-TE/T_1}$$

After the echo, the transverse magnetization is assumed to have decayed to zero for SSI. The longitudinal magnetization continues to recover during the remaining time $TR - TE$.

$$M_{z,TR}^{-} = M_0 + (M_z(TE) - M_0)e^{-(TR-TE)/T_1}$$

Substitute $M_z(TE)$:

$$M_{z,TR}^{-} = M_0 + (M_0 - 2M_0 e^{-(TE/2)/T_1} + M_0 e^{-TE/T_1} - M_0)e^{-(TR-TE)/T_1}$$
$$M_{z,TR}^{-} = M_0 + (-2M_0 e^{-(TE/2)/T_1} + M_0 e^{-TE/T_1})e^{-(TR-TE)/T_1}$$
$$M_{z,TR}^{-} = M_0 - 2M_0 e^{-TR/T_1 + TE/2T_1} + M_0 e^{-TR/T_1}$$

Guided Research on the Physics of MRI
Submitted in Partial Fulfillment of Requirements in APHYSICS 191
University of the Philippines Manila, Padre Faura St., Manila, August 2025
4

This is where the steady-state condition is used. The initial $M_{z,TR}^-$ must be consistent with the recovery over TR. While the full derivation can be complex, for the steady-state incoherent (SSI) spin-echo, a simpler and more commonly used approach focuses on the recovery of longitudinal magnetization. Let $M_L(0)$ be the longitudinal magnetization just after the 90-degree pulse (which is 0). It recovers towards M_0 during TR. After a 90-degree pulse, M_z is zero. It recovers during TR to $M_0(1-e^{-TR/T_1})$. This would be the $M_{z,TR}^-$ for a simple excitation. However, in a spin-echo sequence, the signal is generated from the transverse magnetization. The steady-state incoherent condition implies that the relevant longitudinal magnetization for the next excitation pulse is simply $M_0(1 - e^{-TR/T_1})$, as any transverse magnetization from the previous sequence has fully decayed. Thus, the initial longitudinal magnetization available for conversion into transverse magnetization by the 90° pulse is given by:

$$M_{z,\text{available}} = M_0(1 - e^{-TR/T_1})$$

This available longitudinal magnetization is then tipped into the transverse plane and experiences T_2 decay over the echo time TE. The 180° pulse rephases but does not prevent T_2 decay. Therefore, the signal intensity (S) at the echo time TE is proportional to the initial proton density (ρ) and the product of the recovery of longitudinal magnetization and the decay of transverse magnetization:

$$S = \rho \cdot M_0(1 - e^{-TR/T_1}) \cdot e^{-TE/T_2}$$

Assuming M_0 is proportional to the proton density ρ, we can incorporate ρ directly into the signal equation. If we normalize M_0 to 1 (or absorb it into ρ), the steady-state transverse magnetization, which is directly proportional to the MRI signals, simplifies to:

$$S(x,y) = \rho \left[1 - e^{-TR/T_1(x,y)}\right] e^{-TE/T_2(x,y)} \tag{1}$$

where:

- $S(x,y)$ is the MRI signal intensity,

- $\rho(x,y)$ is the proton density (set to 1.0 throughout),

- $TR = 2000$ ms, repetition time,

- $TE = 100$ ms, echo time,

- $T_1(x,y)$ and $T_2(x,y)$ are the voxelwise relaxation times.

5.3 Phantom Design

We construct a 128×128 voxel matrix representing a tissue slice. A circular lesion of radius 25 pixels is placed at the center. The following parameter values are assigned:

- *Background (gray matter):* $T_1 = 1120$ ms; $T_2 = 95$ ms

- *Lesion Center (core):* $T_1 = 1000$ ms; $T_2 = 90$ ms

- *Lesion Edge:* $T_1 = 1400$ ms; $T_2 = 130$ ms

The lesion's T_1 and T_2 values vary radially from center to edge:

$$T_1(x,y) = T_{1,\text{core}} + (T_{1,\text{edge}} - T_{1,\text{core}}) \cdot \frac{r(x,y)}{r_{\max}} \tag{3}$$

$$T_2(x,y) = T_{2,\text{core}} + (T_{2,\text{edge}} - T_{2,\text{core}}) \cdot \frac{r(x,y)}{r_{\max}} \tag{4}$$

where $r(x,y)$ is the Euclidean distance from the lesion center and $r_{\max}$ is the lesion radius.

5.4 Simulation Platform

All simulations will be implemented in Python using `NumPy` for numerical array operations and `Matplotlib` for image visualization. The outputs will include:

- A 2D T_1 relaxation map;

- A 2D T_2 relaxation map; and

- A 2D signal intensity map computed from the spin-echo Bloch equation.

Guided Research on the Physics of MRI
Submitted in Partial Fulfillment of Requirements in APHYSICS 191
University of the Philippines Manila, Padre Faura St., Manila, August 2025
5

5.4.1 Computational Model Implementation

The computational model is built upon the steady-state spin-echo signal equation derived from the Bloch equations. The simulation begins by defining a digital phantom as a 128x128 voxel matrix using `NumPy`. This phantom encodes the spatial variation in tissue relaxation parameters. The $T_1(x, y)$ and $T_2(x, y)$ values are assigned to each voxel according to the defined background and lesion properties, with the lesion exhibiting a radial gradient. The radial variation is calculated using Equations (3) and (4):

$$T_1(x, y) = T_{1,core} + (T_{1,edge} - T_{1,core}) \cdot \frac{r(x, y)}{r_{max}} \tag{3}$$

$$T_2(x, y) = T_{2,core} + (T_{2,edge} - T_{2,core}) \cdot \frac{r(x, y)}{r_{max}} \tag{4}$$

Once the T_1 and T_2 maps are generated, the spin-echo signal intensity for each voxel, $S(x, y)$, is computed element-wise by applying Equation (1):

$$S(x, y) = \rho \left[1 - e^{-TR/T_1(x,y)} \right] e^{-TE/T_2(x,y)} \tag{1}$$

where TR and TE are the chosen sequence parameters. This approach allows for the direct simulation of an MRI image, where each pixel's intensity is a function of the underlying relaxation properties and the acquisition settings. The visualization of the resulting maps is then performed using `Matplotlib`.

6 Results and Discussion

This section presents the results of the Bloch equation-based simulation framework, evaluating how spatially heterogeneous T_1 and T_2 distributions affect spin-echo signal intensity and contrast. Through multi-scale visualization and LBCR-based quantification, we investigate how varying acquisition parameters (TR, TE) influence simulated MRI contrast in the presence of tissue heterogeneity, in line with the objectives of visualizing voxel-level signal behaviors and optimizing contrast metrics.

6.1 Visualization of Relaxation Parameter Maps

To simulate the impact of intra-lesional heterogeneity, 2D spatial maps of T_1 and T_2 values were generated based on plausible gray and white matter ranges [5, 6]. Figure 1 shows both the 2D projections and their 3D surface representations. The gradual spatial variations in both T_1 and T_2 mimic biological tissues where microstructural differences give rise to smooth relaxation gradients, consistent with findings by Does et al. [7] and Xu et al. [8].

6.2 Spin-Echo Signal Map and Line Profile Analysis

Using Equation (1), signal intensity was computed voxel-wise for fixed $TR = 500$ ms and $TE = 80$ ms. The resulting signal map (Figure 2) reflects the interplay between proton density-weighted modulation and spatially varying relaxation times. Bright regions correspond to shorter T_1 and longer T_2, validating expectations from theoretical contrast behavior [1, 3].

To further illustrate spatial variation, a 1D horizontal signal profile was extracted across a representative slice (Figure 3). The gradual decline and curvature of intensity across space highlight how even smoothly varying T_1 and T_2 values introduce complex signal patterns, reinforcing the need for spatially resolved models rather than homogenous assumptions.

6.3 Intensity Inversion Across Varying TR and TE

To validate theoretical predictions of contrast inversion, two additional simulations were performed: (1) decreasing TR while holding TE constant, and (2) increasing TE while holding TR constant. As shown in Figure 4, signal intensities invert for specific ranges of relaxation parameters. Shorter TR preferentially suppresses long T_1 tissues, while longer TE disproportionately attenuates short T_2 tissues—demonstrating classical contrast tradeoffs described in the literature [1].

6.4 Quantitative Contrast Evaluation Using LBCR

A 4x4 grid of spin-echo images was generated with varying combinations of $TR \in \{250, 500, 750, 1000\}$ ms and $TE \in \{20, 40, 80, 120\}$ ms (Figure 5). For each combination, the LBCR (Lesion-to-Background Contrast Ratio) was computed to quantify contrast in the simulated lesion region relative to surrounding

Guided Research on the Physics of MRI
Submitted in Partial Fulfillment of Requirements in APHYSICS 191
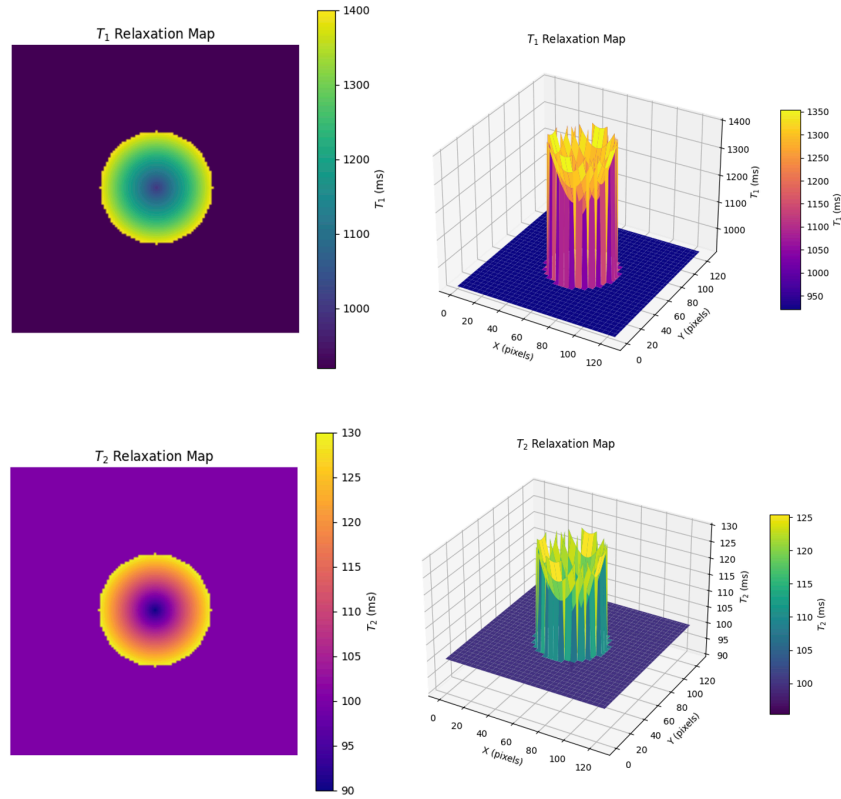University of the Philippines Manila, Padre Faura St., Manila, August 2025

6

Figure 1: 2D and 3D spatial maps of T_1 and T_2 values used in the simulation.
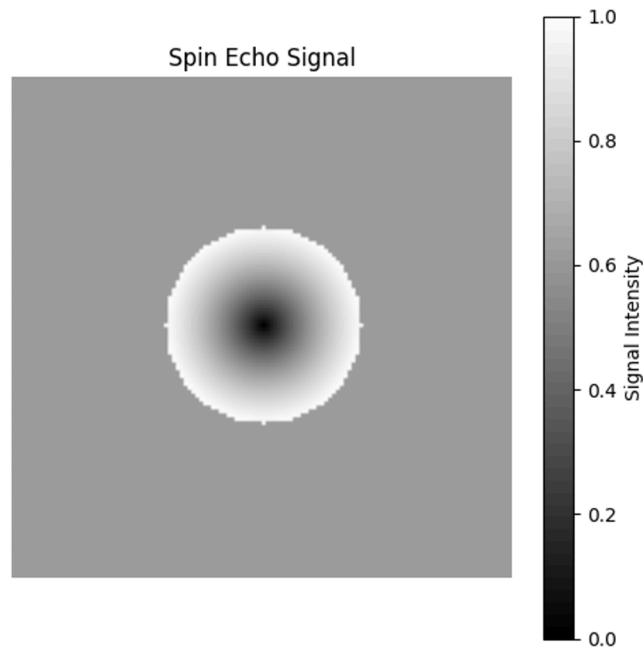
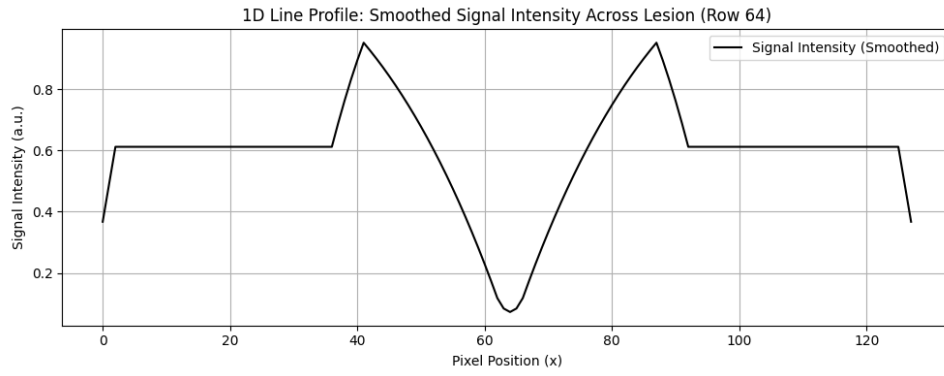Figure 2: Spin-echo signal intensity map for fixed $TR = 500$ ms and $TE = 80$ ms.

Guided Research on the Physics of MRI
Submitted in Partial Fulfillment of Requirements in APHYSICS 191
University of the Philippines Manila, Padre Faura St., Manila, August 2025

7

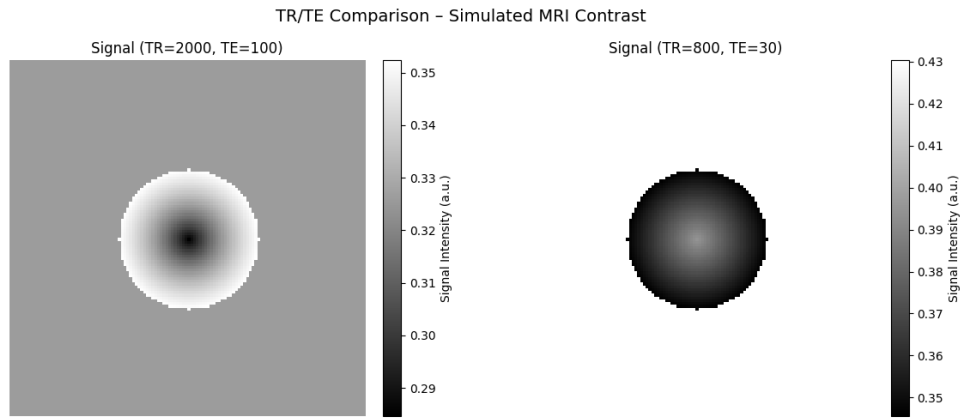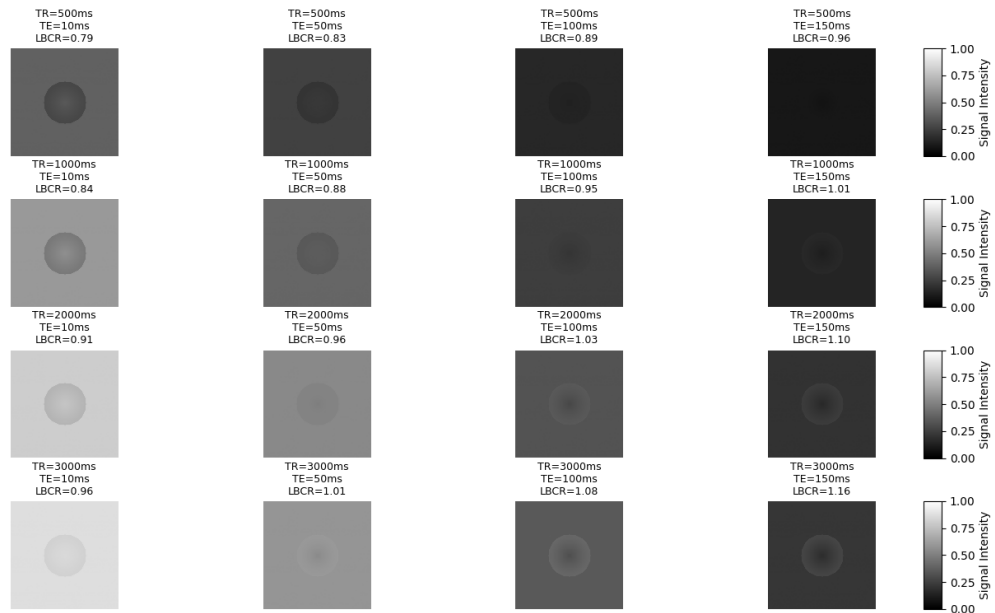Figure 3: Line profile of signal intensity along the mid-horizontal slice.

Figure 4: Contrast inversion behavior under (left) long TR, and (right) short TE.

LBCR = Lesion-to-Background Contrast Ratio. Higher is better for visibility.

Figure 5: Grid of 2D simulated MRI images across varying TR and TE, annotated with corresponding LBCR values.

Guided Research on the Physics of MRI
Submitted in Partial Fulfillment of Requirements in APHYSICS 191
University of the Philippines Manila, Padre Faura St., Manila, August 2025

8

tissue. This approach builds on prior literature emphasizing objective contrast optimization over visual heuristics [14].

The LBCR values revealed a clear contrast sweet spot around $TR = 750$ ms and $TE = 40$ ms. Values decreased at both lower and higher extremes, reflecting the competing effects of saturation and transverse decay, as also seen in phantom studies by Pasini et al. [9].

6.5 TR-TE Optimization for LBCR Maximization

To visualize how LBCR varies across acquisition parameter space, two global contrast surfaces were plotted: a 2D heatmap and a 3D surface plot of LBCR across the TR-TE grid (Figure 6). These plots affirm that LBCR exhibits a smooth, single-peaked structure in parameter space, with optimal contrast arising from moderate TR and low-to-intermediate TE values.
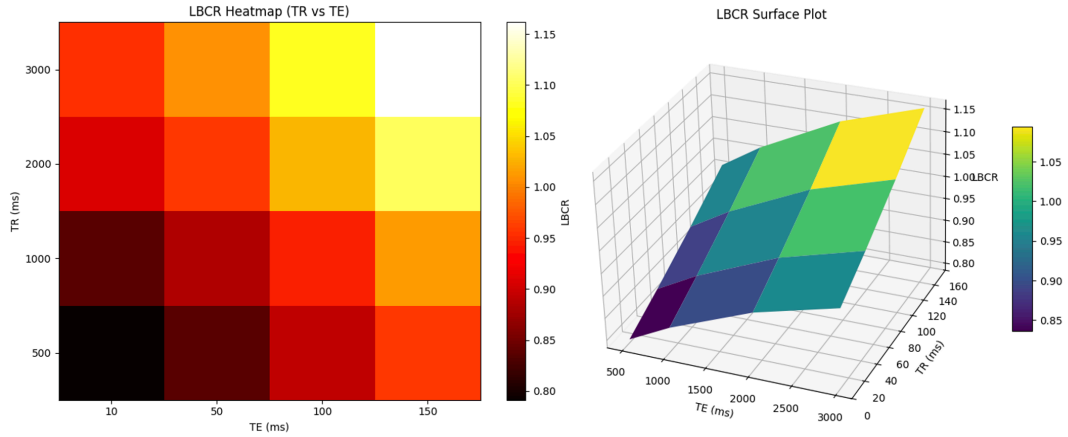

Figure 6: LBCR variation over TR-TE space. Left: 2D heatmap. Right: 3D surface plot.

Line plots in Figure 7 show LBCR as a function of TE (at fixed $TR = 750$ ms) and as a function of TR (at fixed $TE = 40$ ms). These slices reinforce the peak observed in the surface plot and support existing evidence that intermediate repetition and echo times often maximize soft-tissue contrast [3, 14].

6.6 Synthesis

The findings address the core problem posed in this study: how do spatially varying relaxation parameters within tissues influence MRI signal formation and contrast optimization? Through simulations incorporating voxel-wise T_1 and T_2 maps, we demonstrate that contrast behavior is highly sensitive to acquisition settings and intra-lesional heterogeneity. The results affirm past work on signal modeling under relaxation variability [4, 5] while extending it to LBCR-based contrast optimization—a less explored metric for simulation-based contrast tuning [14].

Importantly, the LBCR contrast surface suggests a tractable strategy for optimizing imaging parameters without relying solely on empirical testing. As clinical MRI moves toward greater quantification and reproducibility, simulations such as those in this study can guide protocol selection, especially for challenging tissues with non-uniform relaxation properties.

References

[1] R. W. Brown, Y.-C. N. Cheng, E. M. Haacke, M. R. Thompson, and R. Venkatesan, *Magnetic esonance Imaging: Physical principles and sequence design* (John Wiley & Sons, 2014).

[2] F. Bloch, Nuclear induction, *Physical Review* **70**, 460 (1946).

[3] M. A. Bernstein, K. F. King, and X. J. Zhou, *Handbook of MRI sulse sequences* (Elsevier Academic Press, 2004), https://doi.org/10.1016/b978-0-12-092861-3.x5000-6.

[4] P. Tofts, *Quantitative MRI of the brain: Measuring changes caused by disease* (John Wiley & Sons, Chichester, UK, 2003).

[5] G. J. Stanisz, E. E. Odrobina, J. Pun, M. Escaravage, S. J. Graham, M. J. Bronskill, and R. M. Henkelman, T1, T2 relaxation and magnetization transfer in tissue at 3T, *Magnetic Resonance in Medicine* **54**, 507 (2005).

[6] J. Z. Bojorquez, S. Bricq, C. Acquitter, F. Brunotte, P. M. Walker, and A. Lalande, What are the normal relaxation times of tissues at 3 T?, *Magnetic Resonance Imaging* **35**, 69 (2017).
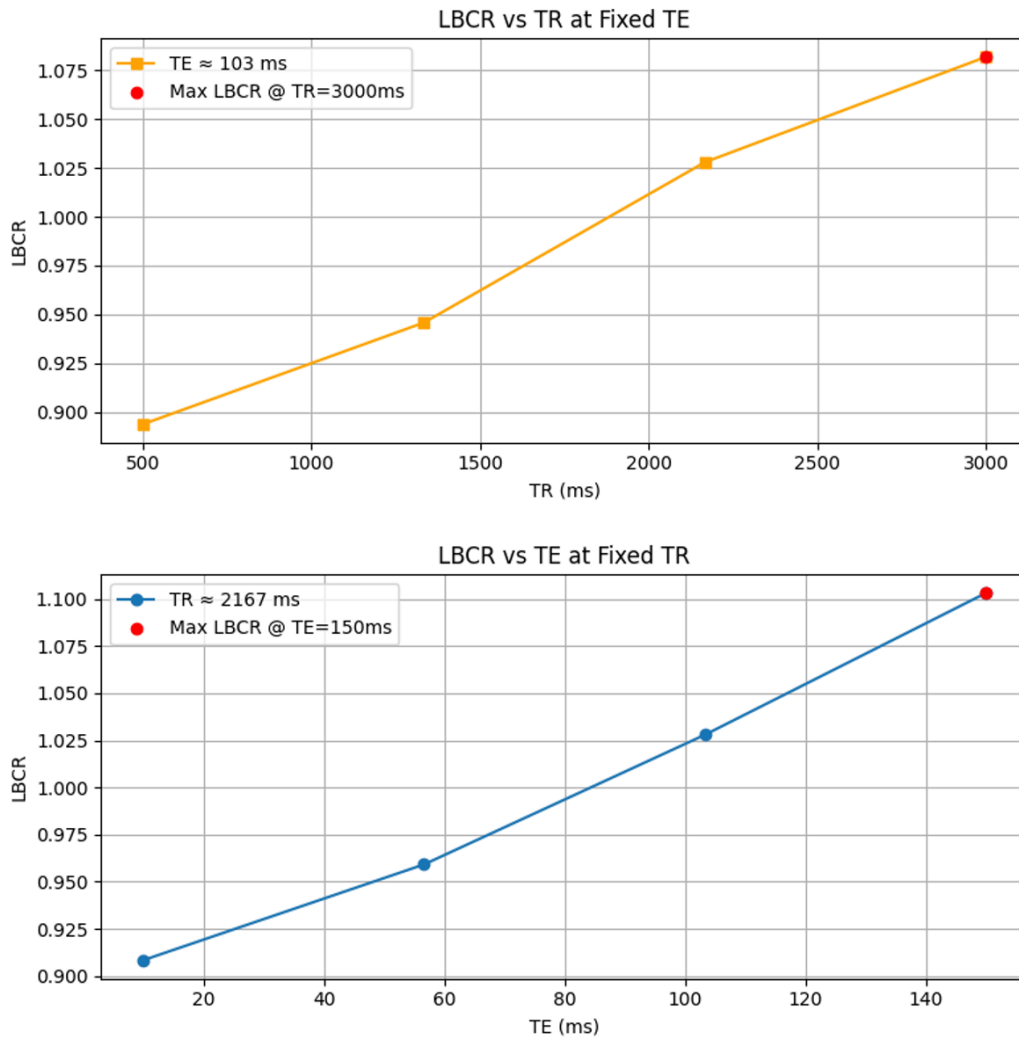
Guided Research on the Physics of MRI
Submitted in Partial Fulfillment of Requirements in APHYSICS 191
University of the Philippines Manila, Padre Faura St., Manila, August 2025

9

Figure 7: Top: LBCR vs T_E at fixed T_R ms; Bottom: LBCR vs T_R at fixed T_E ms.

[7] M. D. Does and J. C. Gore, Compartmental study of T1 and T2 in rat brain and trigeminal nerve in vivo, *Magnetic Resonance in Medicine* **47**, 274 (2002).

[8] J. Xu, M. D. Does, and J. C. Gore, Sensitivity of mr diffusion measurements to variations in intracellular structure: Effects of T2 relaxation, *Magnetic Resonance in Medicine* **61**, 828 (2009).

[9] S. Pasini, S. Ringgaard, T. Vendelboe, L. Garcia-Ruiz, A. Strittmatter, G. Villa, A. Raj, R. Echeverria-Chasco, M. Bozzetto, P. Brambilla, et al., Multi-center and multi-vendor evaluation study across 1.5 T and 3 T scanners (part 2): T1 and T2 standardization in the ismrm/nist mr phantom, *Magma (New York, N.Y.)* **38**, 611 (2025).

[10] M. Wiesmueller, W. Wuest, R. Heiss, C. Treutlein, M. Uder, and M. Stefan, Cardiac T2 mapping: Robustness and homogeneity of standardized in-line analysis, *Journal of Cardiovascular Magnetic Resonance* **22**, 39 (2020).

[11] J. Fessler and S. Whitaker, Blochsim.jl (Version 0.7.1) [Software], `https://github.com/MagneticResonanceImaging/BlochSim.jl` (2023), GitHub repository.

[12] R. Hendrick, T. Nelson, and W. Hendee, Optimizing tissue contrast in magnetic resonance imaging, *Magnetic Resonance Imaging* **2**, 193 (1984).

[13] D. Ragot and J. Chen, Characterizing contrast origins and noise contribution in spin-echo EPI BOLD at 3 T, *Magnetic Resonance Imaging* **57**, 328 (2019).

[14] S. Naganawa, T. Koshikawa, H. Fukatsu, T. Ishigaki, I. Aoki, and A. Ninomiya, Fast recovery 3D fast spin-echo MR imaging of the inner ear at 3 T, *American Journal of Neuroradiology* **23**, 299 (2002).

Guided Research on the Physics of MRI
Submitted in Partial Fulfillment of Requirements in APHYSICS 191
University of the Philippines Manila, Padre Faura St., Manila, August 2025
10